Master of Science
Materials Science

Project Report

The influence of Convection on the Evolution of Microstructure during Solidification

Submitted By:-
Apaar Shanker
(SR No. 09101)

Under the guidance of
Dr. Abhik Choudhury

Contents

Synopsis

Solidification is one of the major materials processing techniques, where in there is a phase transformation from a liquid to one or more solid phases. The process gives rise to a variety of microstructures - arising out of dendritic, eutectic, peritectic and monotectic reactions.

It is well known that properties of a material can be linked to its structure at the microscopic scale. Thus, in order to manufacture a cast product with desired properties, it is essential to determine the influence of the processing parameters on microstructural evolution. Here, simulations of computational models for solidification allow for the determination of the useful process $\rightarrow$ structure and parameter $\rightarrow$ structure correlations while saving up on the time, efforts and material costs required in manual determination of the same.

Solidification, a first order phase transition, involves a transfer of heat/mass across the interface between the solid and the liquid phases concomitant with diffusion in the bulk liquid and the solid phases. Any modeling technique describing this phenomenon will require, that in addition to the global boundary conditions controlling the heat/mass exchange, it self-consistently is able to integrate the transport processes at the moving interface with those in the bulk.

Classically, such problems were treated with ***Sharp-interface*** methods, wherein, separate transport equations are solved in the respective bulk phases, while the appropriate (*Stefan-boundary*) conditions are imposed at the interface nodes which therefore need to be marked after each time iteration. The method becomes cumbersome in case of complex morphological evolution which is commonly encountered in most solidification reactions, where explicit interface tracking becomes computationally expensive and resolving sharp curvatures necessitates the use of finer meshes.

In this context, we resort to the ***phase field method*** - a state-of-the art technique, developed over the past three decades which obviates the need for tracking of the moving interfaces. Succinctly, the method describes evolution equations for order parameters varying smoothly between the various phases, thereby representing phase evolution. The various boundary conditions at the moving interface are self-consistently described in the transport equations describing solutal/heat/momentum transport, which are defined globally. The transport equations are coupled with the evolution equations for the order parameter.

This class of methods has been applied to a variety of phase transformation reactions.

Presently, we have used the phase field method to investigate the ***influence of convection on dendritic growth***. There is a large practical interest in dendritic solidification as an overwhelming majority of metallic systems solidify in this manner. This is also an interesting problem in terms of understanding the mechanisms of pattern selection in non-equilibrium systems and engenders a lot of theoretical interest.

In practical set-ups the dendritic growth is unavoidably influenced by either buoyancy driven natural convection or via forced flows(stirring) in the melt phase, causing large scale transport of mass or heat. This effect of advection due to fluid flow on the evolving dendrite's morphology, has not yet been fully understand and is of great practical importance.

In the present study we have endeavored to throw some light this aspect of solidification. We have set up a phase field model to simulate dendritic growth. To this, we have coupled fluid solvers, which are based on -

1. Direct numerical simulation of the navier stokes equations.
2. Lattice Boltzmann-BGK model

We thus seek to directly simulate dendritic growth in a convective regime and gauge the effect of flow on the evolving morphology of the solid phase.

An introduction to Dendritic Solidification

Dendritic solidification is ubiquitous in nature and is of great practical and theoretical importance. The dendritic morphology can be characterised by growth of primary arms along well defined crystallographic directions with each primary arm also giving rise to self-similar secondary and tertiary arms.

Dendritic microstructures result as a destabilization of a planar or spherical growth front. A critical component giving rise to dendritic morphology, where the primary growth occurs along well defined directions, is the surface energy anisotropy.

Physically, an understanding of dendrite morphology and growth would entail the knowledge of the scaling laws pertaining to - dendrite tip radius, inter dendritic and secondary arm spacings and how they change as a function of the processing conditions, alloy composition and properties. The requirement for understanding the scale and variation of these parameters lies in the fact that macroscopic parameters such as tensile strength, fracture toughness etc. are often determined by the scale of the microstructure.

There have been significant advances in understanding the physics of dendritic growth. The role of crystalline anisotropy in the selection of the dendrite tip radius and velocity is well explained by the microsolvability theory [1]. The theory has been validated by sophisticated micro gravity experiments as well as phase field simulations in both two and three dimensions, that focused on the purely diffusive regime.

On earth, however, dendritic growth is almost unavoidably influenced by buoyancy driven mass and energy advection in the melt phase. Melt flow introduces a new length scale in the problem, viz. the length of the convecting rolls, and breaks the symmetry of transport depending on the direction of the vector of gravity relative to the direction of growth. Self-organizing pattern formation in solidification begins to compete with the self-organization of the convection patterns. On the one hand, convective transport of solute significantly alters the growth conditions. On the other hand, the magnitude of convection critically depends on solute gradients due to growth and on the friction of the convecting liquid melt against the growing solid-liquid interface[3].

A Phase Field Model for Solidification

3.1 The Phase Field Method

In the phase field method the system properties are expressed using a set of phasefield variables that vary continuously within a bound across all the phases in the system. The thermodynamics and transport properties of the system are coupled with or expressed in terms of the dynamics of these phasefield variables.

The time evolution of the phase field variables is given by a set of coupled partial differential equations, one equation for each variable. The equations are derived according to the principles of non-equilibrium thermodynamics.They are so chosen that the free energy of the system decreases with time and mass is conserved for all components. Likewise transport properties within the bulk as well as the interface are incorporated to be consistent with the dynamics of these phasefield variables. Numerical solutions of these PDE's yield the temporal evolution of the phasefield variables, which is a representation of the morphological evolution of the "phases" in the system.

The application of the phase field method starts with the creation of a functional which includes the material properties - the surface energies of the interfaces and the thermodynamic free energies of the bulk phases in the system. A variational derivative of this functional with respect to any of the phasefield variables, gives us the dynamics vis-a-vis that variable.

3.2 The Allen-Cahn Equation

We need to come up with an equation that encompasses the energetics of the system. We can start with the energy density functional for an equilibrium state ϕ_o and add energy contributions with respect to the variation from this state. This construction, would write as,

$$f\left(\phi, \nabla\phi, \nabla^2\phi\right) = f_o\left(\phi\right) + \frac{\partial f}{\partial \phi'}\delta\phi' + \frac{\partial f}{\partial \phi''}\delta\phi'' + \frac{1}{2}\frac{\partial f}{\partial^2 \phi'}\left(\delta\phi'\right)^2 \tag{3.1}$$

The energy state of the system cannot depend on the choice of the coordinate system should be rotationally invariant. This can be guaranteed only if $\frac{\partial f}{\partial \phi' \delta\phi'}$ makes zero

contribution to the energy integral. Therefore, the simplest energy density that can be written takes the following form,

$$f\left(\phi, \nabla\phi\right) = f_o\left(\phi\right) + \kappa_1\left(\nabla\phi\right)^2 + \kappa_2\left(\nabla^2\phi\right) \tag{3.2}$$

The total energy of the system is a volume integral of the energy density and after some more simplification can be written down in the functional form as,

$$\mathcal{F} = \int_{-\infty}^{\infty}\left(f_o\left(\phi\right) + \kappa\left(\nabla\phi\right)^2\right)dV \tag{3.3}$$

If we were, to compute the time-derivative of the change in the free-energy functional, it can be written as,

$$\frac{\delta\mathcal{F}}{\delta t} = \int_{-\infty}^{\infty}\frac{\delta\mathcal{F}}{\delta\phi}\frac{\partial\phi}{\partial t}dx \tag{3.4}$$

Given that ϕ is a non conserved variable, the simplest way to ensure that the functional is minimised in time, would be,

$$\frac{\partial\phi}{\partial t} = -M\frac{\delta\mathcal{F}}{\delta\phi}, \tag{3.5}$$

such that the time derivative of the free-energy functional now reads,

$$\frac{\delta\mathcal{F}}{\delta t} = -\int_{-\infty}^{\infty}M\left(\frac{\delta\mathcal{F}}{\delta\phi}\right)^2 dx. \tag{3.6}$$

Clearly, here, we are minimizing the energy. However, the rate of change is zero, when the functional is at an extremum given by $\dfrac{\delta\mathcal{F}}{\delta\phi} = 0$.

The dynamical evolution for ϕ is then expressed as,

$$\frac{\partial\phi}{\partial t} = -M\frac{\delta F}{\delta\phi}. \tag{3.7}$$

where $\dfrac{\partial}{\partial t}$ is operator for variational derivative and expands as,

$$\frac{\delta\mathcal{F}}{\delta\phi} = \left(\frac{\partial}{\partial\phi} - \nabla\cdot\frac{\partial}{\partial\nabla\phi} + \nabla^2\cdot\frac{\partial}{\partial\nabla^2\phi}\ldots\right)f \tag{3.8}$$

Applying this, we derive,

$$\frac{\partial\phi}{\partial t} = -M\left(\frac{\partial f_o}{\partial\phi} - 2\kappa\nabla^2\phi\right). \tag{3.9}$$

This is the equation describing Allen-Cahn dynamics and is applicable to a large class of materials transformations, for example, evolution of grain-boundaries, order-disorder transitions, solidification etc.

3.3 Modelling Alloy Solidification

We have in the previous section derived the Allen-Cahn equation, where in, if the two phases have the same free energy, a stationary interface with a defined width is created. However, if we were to add a term to the energy functional such that it tilts one of the energy levels with respect to the other, the phenomenological equation of motion, has so been constructed that the evolution of ϕ will be in a direction such that the phase with the higher energy will be consumed in favour of the phase with the lower energy.

This then is an apt recipe for modelling solidification. Formally this tilting, or rather the departure from equilibrium between the two phases, can be expressed as the *driving force* for phase transformation. In the case of solidification of binary isomorphous alloy, at a given under cooling, the driving force arises due to deviation of the diffusion potential from the equilibrium and results in solute rejection at the interface and expansion of the solidification front.

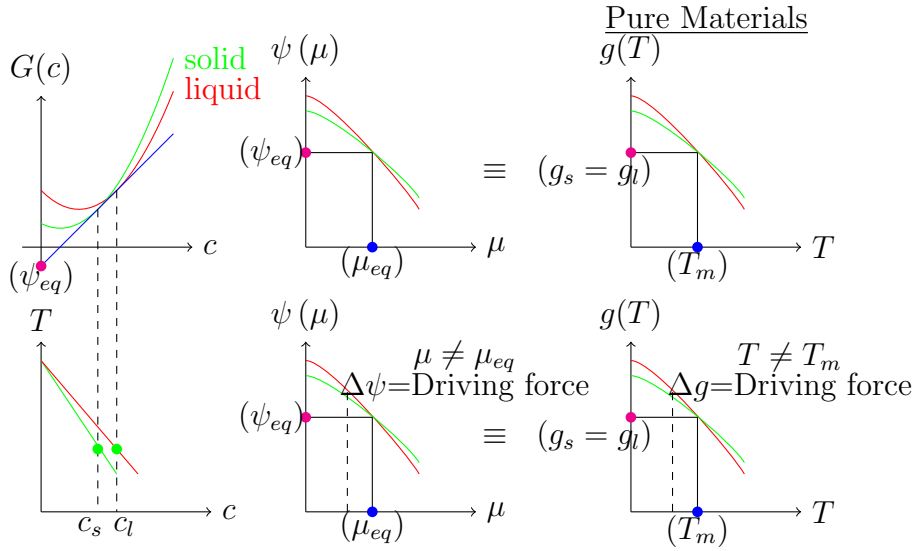

Assuming conditions of local thermodynamic equilibrium(LTE), the driving force for phase transformation in alloys is the difference of the grand-potentials of the solid and the liquid phases (or the difference of the chemical potentials of any of the chemical entities depending on whether we start from a Helmholtz free-energy density or a Gibbs-free energy density in the functional).

In the present description, we adopt a Helmholtz free energy density. This treatment has been referenced from the work of Abhik N. Chaudhary [5]. The driving force for solidification can be described as $\Psi_l - \Psi_s$ This is analogous to the case of pure material solidification where the driving force is given by $g_l - g_s$. However, while the state-variable in the case of pure material solidification is the temperature T, it becomes the diffusion-potential μ in the case of binary alloy solidification. This analogy can be well appreciated from the diagram in Fig 3.3.

At equilibrium, the common-tangent construction gives the equilibrium compositions of the solid and liquid phases, which can be read from the equilibrium phase diagram. This same equilibrium can also be represented as the intersection of the grand-potential densi-

ties $\Psi(\mu)$ expressed as a function of the diffusion-potentials μ, where $\Psi_s(\mu_{eq}) = \Psi_l(\mu_{eq})$, in the same manner as $g_s(T_m) = g_l(T_m)$ for the case of pure materials. Away from equilibrium $\mu \neq \mu_{eq}, \Psi_l \neq \Psi_s$, and we have a driving force for phase transition given by the difference of the grand-potential densities.

Therefore, using this above analogy we can write down the driving force for phase transition for alloys purely in terms of the diffusion potential μ by performing a Taylor series expansion around equilibrium, until the first order as follows,

$$\Psi_s(\mu) = \Psi_s(\mu_{eq}) + \frac{\partial \Psi_s}{\partial \mu}(\mu - \mu_{eq}) \tag{3.10}$$

$$\Psi_l(\mu) = \Psi_l(\mu_{eq}) + \frac{\partial \Psi_l}{\partial \mu}(\mu - \mu_{eq}). \tag{3.11}$$

From the fig. 3.3 it is clear that we can express the grand-potential as $\Psi(\mu) = g(c(\mu)) - \mu c(\mu)$, which is the essentially the *Legendre transform* of g. Therefore, we can derive,

$$\begin{aligned}\frac{\partial \Psi}{\partial \mu} &= \frac{\partial g}{\partial c}\frac{\partial c}{\partial \mu} - \mu\frac{\partial c}{\partial \mu} - c \\ &= -c,\end{aligned}$$

where we have used $\dfrac{\partial g}{\partial c} = \mu$. Clearly, then we can write the driving force for solidification $\Psi_l - \Psi_s$ as,

$$\Psi_l - \Psi_s = (c_s^{eq} - c_l^{eq})(\mu - \mu_{eq}), \tag{3.12}$$

where we have used $\Psi_l(\mu_{eq}) = \Psi_s(\mu_{eq})$ and $\left.\dfrac{\partial \Psi_l}{\partial \mu}\right|_{\mu_{eq}} = -c_l^{eq}$ and $\left.\dfrac{\partial \Psi_s}{\partial \mu}\right|_{\mu_{eq}} = -c_s^{eq}$. This relation can be transmitted to the evolution equation for the phase-field variable ϕ as,

$$\frac{\partial \phi}{\partial t} = -M\left(\frac{\partial f_o}{\partial \phi} - 2\kappa\nabla^2\phi\right) - M\underbrace{(c_l^{eq} - c_s^{eq})(\mu - \mu_{eq})\frac{\partial h(\phi)}{\partial \phi}}_{driving force}. \tag{3.13}$$

The evolution equation of the coupled variable μ can be derived using mass conservation. Using the interpolation polynomial $h(\phi) = \phi^2(3 - 2\phi)$, which has the property $h(\phi) + h(1-\phi) = 1$, the local composition can be written as,

$$c = c_s h(\phi) + c_l(1 - h(\phi)), \tag{3.14}$$

Now the mass conservation equation can be written as,

$$\frac{dc}{dt} = \nabla \cdot (M\nabla\mu) \tag{3.15}$$

Also, (3.16)

$$\frac{dc}{dt} = \frac{\partial c}{\partial t} + \frac{\partial c}{\partial x}\frac{\partial x}{\partial t} + \frac{\partial c}{\partial y}\frac{\partial y}{\partial t} + \frac{\partial c}{\partial z}\frac{\partial z}{\partial t} = \frac{\partial c}{\partial t} + \vec{v}\cdot\nabla c \tag{3.17}$$

Thus, we have, (3.18)

$$\frac{\partial c}{\partial t} = \nabla \cdot (M\nabla\mu) - \vec{v}\cdot\nabla c \tag{3.19}$$

Considering, concentrations (c_s&c_l) as a function of diffusion potential (μ), we can write the followng equation;

$$\left(\frac{\partial c_s}{\partial \mu}h\left(\phi\right)+\frac{\partial c_l}{\partial \mu}(1-h\left(\phi\right))\right)\frac{\partial \mu}{\partial t}=\underbrace{\nabla\cdot\left(M\nabla\mu\right)}_{\text{Diffusive flux}}-\underbrace{\left(c_s\left(\mu\right)-c_l\left(\mu\right)\right)\frac{\partial h\left(\phi\right)}{\partial t}}_{\text{Source term}}-\underbrace{\vec{v}\cdot\nabla c}_{\text{Advective flux}} \tag{3.20}$$

Here, the first term on the right hand side represents the diffusive flux, while the second term is the source term for phase transformation. The third, velocity coupled, term represents mass advection and accounts for influence of melt flow on the morphological evolution.

Thus, we are able to derive the evolution equations for solidification in alloys by starting with a phenomenological model for non conservative dynamics, based on an ansatz, and thereafter deriving the driving force in terms of the relevant state variables and then coupling it with the appropriate conservation equations.

3.4 The phasefield Equations

The dynamical evolution equation for the phasefield variable ϕ is as follows;

$$\frac{\partial \phi}{\partial t}=-M\left(\frac{\partial f_o}{\partial \phi}-2\kappa\nabla^2\phi\right)-M\underbrace{\left(c_l^{eq}-c_s^{eq}\right)\left(\mu-\mu_{eq}\right)\frac{\partial h\left(\phi\right)}{\partial \phi}}_{driving force}. \tag{3.21}$$

which is coupled with the evolution equation for diffusion potential μ as

$$\left(\frac{\partial c_s}{\partial \mu}h\left(\phi\right)+\frac{\partial c_l}{\partial \mu}(1-h\left(\phi\right))\right)\frac{\partial \mu}{\partial t}=\nabla\cdot\left(M\nabla\mu\right)-\left(c_s\left(\mu\right)-c_l\left(\mu\right)\right)\frac{\partial h\left(\phi\right)}{\partial t}-\vec{v}\cdot\nabla c \tag{3.22}$$

For the sake of simplicity, in the present model we choose the following relations of c^s and c^l,

$$c^l\left(\mu\right)=\mu \tag{3.23}$$

$$c^s\left(\mu\right)=kc^l=k\mu \tag{3.24}$$

where **k** is the partition coefficient. Then, the expression for driving force becomes

$$\Psi_l-\Psi_s=\left(c_s^{eq}-c_l^{eq}\right)\left(\mu-\mu_{eq}\right)\Rightarrow\Psi_l-\Psi_s=(k-1)\mu\left(\mu-\mu_{eq}\right) \tag{3.25}$$

The evolution equation for ϕ, thus suitably modified, can be written as,

$$\frac{\partial \phi}{\partial t}=-M\left(\frac{\partial f_o}{\partial \phi}-2\kappa\nabla^2\phi\right)-M\underbrace{(k-1)\mu\left(\mu-\mu_{eq}\right)\frac{\partial h\left(\phi\right)}{\partial \phi}}_{driving force}. \tag{3.26}$$

Also, we consider χ defined as follows,

$$\chi = \left(\frac{\partial c^s}{\partial \mu} h\left(\phi\right) + \frac{\partial c^l}{\partial \mu} (1 - h\left(\phi\right)) \right) \tag{3.27}$$

$$\Rightarrow \chi = 1 + (k-1)\, h\left(\phi\right) \tag{3.28}$$

Then, the evolution equation for μ becomes,

$$\chi \left(\frac{\partial \mu}{\partial t} \right) = \nabla \cdot (M \nabla \mu) - \left(c^s\left(\mu\right) - c^l\left(\mu\right) \right) \frac{\partial h\left(\phi\right)}{\partial t} - \vec{v} \cdot \nabla c \tag{3.29}$$

$$\chi \left(\frac{\partial \mu}{\partial t} \right) = \nabla \cdot (M \nabla \mu) - (k-1)\, \mu \frac{\partial h\left(\phi\right)}{\partial t} - \vec{v} \cdot \nabla c \tag{3.30}$$

For the sake of reiteration, $\phi = 1 \Longrightarrow$ solid and $\phi = 0 \Longrightarrow$ liquid
Also, we have chosen the interpolation function $h(\phi)$ such that,

$$h(\phi) = \phi^2 \left(3 - 2\phi\right) \tag{3.31}$$

$$\frac{\partial h(\phi)}{\partial \phi} = 6\phi \left(1 - \phi\right) \tag{3.32}$$

We chose f_o to be the classic double well potential, given as,

$$f_o = 9\phi^2 \left(1 - \phi\right)^2 \tag{3.33}$$

We also factor in some constants in order to non-dimensionalise the equations: τ as relaxation time and ϵ as relaxation length and γ which corresponds to surface energy. Incorporating all these, the equations for evolution of the field variables can finally be written down as,

$$\tau\epsilon \frac{\partial \phi}{\partial t} = \gamma \nabla^2 \phi - \frac{\gamma}{\epsilon} 18\phi(1-\phi)(1-2\phi) + (k-1)\mu \left(\mu - \mu_{eq}\right) (6\phi) \left(1 - \phi\right) \tag{3.34}$$

$$\chi \frac{\partial \mu}{\partial t} = M \nabla^2 \mu - 6\left(k-1\right) \mu\phi \left(1 - \phi\right) \frac{\partial \phi}{\partial t} - \vec{v} \cdot \nabla c \tag{3.35}$$

3.5 Incorporating Anisotropy

Our free energy functional is of the form,

$$\mathcal{F} = \int_{-\infty}^{\infty} (\gamma\epsilon |\nabla\phi|^2 + \frac{\gamma}{\epsilon} 9\phi^2(1-\phi)^2 + ...) dV \tag{3.36}$$

We define an interfacial energy term with a small cubic anisotropy to the order of a few percent as $a_c = \gamma_o \left(1 - \delta_{\alpha\beta} cos(4\theta)\right)$ where $\delta_{\alpha\beta}$ is the strength of anisotropy.

Accordingly, the functional gets modified to be,

$$\mathcal{F} = \int_{-\infty}^{\infty} (\gamma a_c^2(\theta) |\nabla\phi|^2 + \frac{\gamma}{\epsilon} 9\phi^2(1-\phi)^2 + ...) dV$$

The interfacial energy needs to be a function of interface normal. For this, we determine the following relation between interface normal $\vec{n}$ and θ which is the angle of orientation.

$\theta = tan^{-1}\left(\frac{n_x}{n_y}\right), cos\theta = n_x, sin\theta = n_y,\ \hat{n} = n_x\hat{i} + n_y\hat{j}$
$n_x^2 + n_y^2 = 1$
$\hat{n} = \frac{\nabla\phi}{|\nabla\phi|}, n_x = \frac{\left(\frac{\partial\phi}{\partial x}\right)}{|\nabla\phi|}, n_y = \frac{\left(\frac{\partial\phi}{\partial y}\right)}{|\nabla\phi|}$

We need to able to fully describe the anisotropy in terms of gradients in the ϕ field. To achieve this we resorted to the following treatment,

Expand $cos4\theta$ as,

$cos4\theta + isin4\theta = (cos\theta + isin\theta)^2$
on collecting the real terms we get
$cos4\theta = cos^4\theta + sin^4\theta - {}^4C_2 cos^2\theta sin^2\theta$
$= n_x^4 + n_y^4 - 6n_x^2 n_y^2$

using: $n_x^2 + n_y^2 = 1$
$\Rightarrow cos4\theta = 4(n_x^4 + n_y^4) - 3$
Now, $a_c = \gamma_o\left(1 - \delta_{\alpha\beta}\left(4\left(n_x^4 + n_y^4\right) - 3\right)\right)$

$$a_c = \gamma_o\left(1 - \delta_{\alpha\beta}\left(4\left(\frac{\frac{\partial\phi}{\partial x}^4 + \frac{\partial\phi}{\partial y}^4}{|\nabla\phi|^4}\right) - 3\right)\right)$$

call $\frac{\partial\phi}{\partial x} \rightarrow \phi_x$ and $\frac{\partial\phi}{\partial y} \rightarrow \phi_y$

$$a_c = \gamma_o\left(1 - \delta_{\alpha\beta}\left(4\left(\frac{\phi_x^4 + \phi_y^4}{\left(\phi_x^2 + \phi_y^2\right)^2}\right) - 3\right)\right)$$

The variational derivative operator expands as,

$$\frac{\delta}{\delta\phi} = \left(\frac{\partial}{\partial\phi} - \nabla\phi\cdot\frac{\partial}{\partial\nabla\phi}\right)$$

Then on incorporating anisotropy, the gradient energy term in the evolution equation gets modified as,

$$\frac{\delta}{\delta\phi}\left(a_c^2|\nabla\phi|^2\right) = \frac{\partial}{\partial\phi}\left(a_c^2|\nabla\phi|^2\right) - \nabla\phi\cdot\frac{\partial}{\partial\nabla\phi}\left(a_c^2|\nabla\phi|^2\right)$$

As both a_c and $|\nabla\phi|$ are a function of ϕ_x and ϕ_y only, the $\frac{\partial}{\partial\phi}$ term goes to zero. Also, in Cartesian coordinates $\frac{\partial}{\partial\nabla\phi}$ can be written as,

$$\frac{\partial}{\partial\phi_x}\hat{i} + \frac{\partial}{\partial\phi_y}\hat{j}$$

As such, on including anisotropy the time evolution equation for the phase field variable becomes:

$$\tau\epsilon\frac{\partial\phi}{\partial t} = \gamma\epsilon\nabla\cdot\begin{pmatrix}\frac{\partial}{\partial\phi_x}\left(a_c|\nabla\phi|\right)^2\\ \frac{\partial}{\partial\phi_y}\left(a_c|\nabla\phi|\right)^2\end{pmatrix} - \frac{\gamma}{\epsilon}18\phi(1-\phi)(1-2\phi) + (k-1)\mu\left(\mu-\mu_{eq}\right)6\phi\left(1-\phi\right) \tag{3.37}$$

The individual components of the vector $\begin{pmatrix}\frac{\partial}{\partial\phi_x}\left(a_c|\nabla\phi|\right)^2\\ \frac{\partial}{\partial\phi_y}\left(a_c|\nabla\phi|\right)^2\end{pmatrix}$ when fully expanded look as follows,

$$\frac{\partial}{\partial\phi_x}\left(a_c|\nabla\phi|\right)^2 = 2a_c\phi_x\left(\gamma_o - \frac{16\gamma_o\delta\left(\phi_x^2\phi_y^2-\phi_y^4\right)+4\gamma_o\delta\left(\phi_x^4+\phi_y^4\right)}{\left(\phi_x^2+\phi_y^2\right)^2}+3\delta\right) \tag{3.38}$$

$$\frac{\partial}{\partial\phi_y}\left(a_c|\nabla\phi|\right)^2 = 2a_c\phi_y\left(\gamma_o - \frac{16\gamma_o\delta\left(\phi_y^2\phi_x^2-\phi_x^4\right)+4\gamma_o\delta\left(\phi_y^4+\phi_x 4\right)}{\left(\phi_y^2+\phi_x^2\right)^2}+3\delta\right) \tag{3.39}$$

where, $a_c = \gamma_o\left(1-\delta\left(4\left(\frac{\phi_x^4+\phi_y^4}{\left(\phi_x^2+\phi_y^2\right)^2}\right)\right)\right)$

3.6 Concept of material derivative

Let η be a material property. Then the change in η as an infinitesimally small parcel of fluid moves from position $\vec{r}$ to $\vec{r}+\Delta\vec{r}$ over time Δt is expressed as;

$$\frac{D\eta}{Dt} = \frac{\partial\eta}{\partial t} + \vec{u}\cdot\nabla\eta \tag{3.40}$$

wherein $\frac{D\eta}{Dt}$ is known as the material derivative or total derivative of the property η.

3.7 Incorporating Fluid Flow

The evolution equation for μ, derived from mass conservation, includes a term for advective flux that is long range mass transport due to fluid currents.

$$\chi\frac{\partial\mu}{\partial t} = M\nabla^2\mu - 6\left(k-1\right)\mu\phi\left(1-\phi\right)\frac{\partial\phi}{\partial t} - \vec{v}\cdot\nabla c \tag{3.41}$$

The time evolution of velocity fields incorprated here needs to be determined using using appropriate solvers for flow in the melt phase. In the following chapter we shall look at the implementation of:

- direct numerical simulation of navier stokes equations,
- lattice Boltzmann algorithm

to simulate flow and corresponding advection around the evolving solid phase.

Models for simulating fluid flow

4.1 Navier Stokes equation for incompressible flow in newtonian fluid

Equation of continuity (zero generation) is given as,

$$\frac{\partial \rho}{\partial t} + \vec{\nabla} \cdot (\rho \vec{u}) = 0 \tag{4.1}$$

Also, for an incompressible fluid, the material derivative of density (ρ) is zero, i.e.;

$$\frac{D\rho}{Dt} = \frac{\partial \rho}{\partial t} + \vec{u} \cdot \nabla \rho = 0 \tag{4.2}$$

Using 4.1 and 4.2 we get the following modified form of continuity as;

$$\nabla \cdot \vec{u} = 0 \tag{4.3}$$

Also, the equation for momentum transport is expressed as;

$$\rho \frac{D\vec{u}}{Dt} = -\nabla P + \nu \nabla^2 \vec{u} \tag{4.4}$$

$$\implies \frac{\partial \vec{u}}{\partial t} = -\frac{1}{\rho} \nabla P + \frac{\nu}{\rho} \nabla^2 \vec{u} - \vec{u} \cdot (\nabla \vec{u}) \tag{4.5}$$

The equations needed to be modified to correctly simulate flow around the evolving solid phase, ensuring the no slip condition at the solid-liquid interface. We resorted to a description utilised by Steinbach [3], where in the diffuse interface region is viewed as a rigid porous medium. Here, the usual no-slip condition at the sharp solid-liquid interface is enforced through a varying inter facial force term $(1-\phi)$ in the diffuse interface region.

The continuity and momentum transport equations can then be written, respectively as,

$$\nabla \cdot [(1-\phi)\vec{u}] = 0 \tag{4.6}$$

$$\frac{\partial \vec{u}(1-\phi)}{\partial t} = -(1-\phi)\nabla P + \frac{1}{Re} \nabla^2 \left(\vec{u}(1-\phi)\right) - \vec{u} \cdot \nabla \left(\vec{u}(1-\phi)\right) \tag{4.7}$$

4.1.1 Finite Difference - 2 D - Implementation

We can rewrite the time evolution equation for velocity in descretised form as;

$$\frac{\vec{u_{t+dt}} - \vec{u_t}}{\Delta t} = -(1-\phi)\nabla P + \frac{1}{Re}\nabla^2\left(\vec{u}(1-\phi)\right) - \vec{u}\cdot\nabla\left(\vec{u}(1-\phi)\right) \tag{4.8}$$

Define : $\vec{H} = \frac{1}{Re}\nabla^2\left(\vec{u}(1-\phi)\right) - \vec{u}\cdot\nabla\left(\vec{u}(1-\phi)\right)$

Then, $\frac{\vec{u_{t+dt}} - \vec{u_t}}{\Delta t} = -(1-\phi)\nabla P + \vec{H}$

Taking divergence on both sides, we have;

$$\frac{\nabla\cdot\vec{u_{t+dt}} - \nabla\cdot\vec{u_t}}{\Delta t} = -\nabla\cdot\left[(1-\phi)\nabla P\right] + \nabla\cdot\vec{H} \tag{4.9}$$

Now, we know for continuity(4.3) that at any time, the divergence of velocity field is zero; this gives an equation for the pressure field;

$$\nabla\cdot\left[(1-\phi)\nabla P\right] = \nabla\cdot\vec{H} \tag{4.10}$$

We solve the above equation using gauss-siedel method, to get appropriate pressure field which is then used as an input to calculate the velocity fields in the follwing scalar form of the Navier-Stokes equation for momentum transport.

$$\frac{u_{t+dt} - u_t}{\Delta t} = -(1-\phi)\nabla P + \frac{1}{Re}\nabla^2\left(u(1-\phi)\right) - \vec{u}\cdot\nabla\left(u(1-\phi)\right) \tag{4.11}$$

4.2 Lattice Boltzmann-BGK model

We begin the model description with the Boltzmann transport equation,

$$\frac{\partial f}{\partial t} + \vec{u}\cdot\nabla f = \Omega$$

where f is the particle distribution function, representing the probability of finding a particle with velocity $\vec{v}$ as a function of position in space and time. It can also be construed as the fraction of particles with a particular velocity $\vec{v}$ when the particle density tends to the hydrodynamic limit.

Ω, the collision operator, is in general a complex, non linear integral. However, we utilize a linear approximation around its local equilibrium solution, known as the BGK (Bhatnagar, Gross and Crooks[**?**]) collision operator:

$$\Omega = -\frac{1}{\tau}\left(f - f^{eq}\right)$$

where τ is the relaxation time towards the lcoal equilibrium and f^{eq} is the equilibrium particle distribution function. After introducing the BGK approximation, the Boltzmann equation can be written as

$$\frac{\partial f}{\partial t} + \vec{u}\cdot\nabla f = -\frac{1}{\tau}\left(f - f^{eq}\right)$$

4.2.1 Descretised Representation

For a two dimensional representation over a square grid, the probability distribution function is descretised in the following manner.

Particles are restricted to stream in eight possible directions towards the nearest neighbour nodes or stay at rest, resulting in nine possible velocities (including zero), reffered to as the *microscopic velocities* $\vec{e_k}$'s, given as;

Put Grid Image Here

$$\vec{e_i} = \begin{cases} (0,0) & i = 0 \\ (1,0),(0,1),(-1,0),(0,-1) & i = 1,2,3,4 \\ (1,1),(-1,1),(-1,-1),(1,-1) & i = 5,6,7,8 \end{cases}$$

The Boltzmann transport equation, described before, for velocity in a particular direction can be written as;

$$\frac{\partial f_k}{\partial t} + \vec{e_k} \cdot \nabla f = -\frac{1}{\tau}\left(f_k - f^{eq}\right) \tag{4.12}$$

Given time step Δt and space step Δx_k, the above equation can be rewritten in descretised form as;

$$\underbrace{f_i\left(\vec{x} + c\vec{e_i}\Delta t, t + \Delta t\right) - f_i\left(\vec{x}, t\right)}_{\text{Streaming}} = \underbrace{-\frac{\left|f_i\left(\vec{x}, t\right) - f_i^{eq}\left(\vec{x}, t\right)\right|}{\tau}}_{\text{Collision}} \tag{4.13}$$

This equation is implemented in two parts:

- **collision step**: $\tilde{f}_k\left(\vec{x_k}, t + \Delta t\right) = f_k\left(\vec{x_k}, t\right) - \dfrac{\Delta t}{\tau}\left(f_k - f_k^{eq}\right)$
- **streaming step**: $f_k\left(\vec{x_k} + \vec{e_k}\Delta t, t + \Delta t\right) = \tilde{f}_k\left(\vec{x_k}, t + \Delta t\right)$

The combination of e_k, Δx_k and Δt are such that over each time step, $e_k \Delta t$ corresponds to the position of nearest neighbour nodes.

4.2.2 Equilibrium distribution function

The equilibrium distribution function f^{eq} which appears in the BGK collision operator is basically an expansion of the Maxwell-Boltzmann distribution function for small velocities.

$$f = \frac{\rho}{2\pi/3} e^{-\frac{3}{2}(\vec{e}-\vec{u})^2} = \frac{\rho}{2\pi/3} e^{-\frac{3}{2}(\vec{e}\cdot\vec{e})} e^{\frac{3}{2}(2\vec{e}\cdot\vec{u}-\vec{u}\cdot\vec{u})} \tag{4.14}$$

where $\vec{u}$ is the macroscopic velocity of particles, $\vec{e}$ are the velocity vectors in specific model and ρ si the macroscopic mass density.

Now, we expand the above equation for small velocities $M = \frac{u}{c_s} << 1$. [M is the mach number and $c_s = \frac{1}{\sqrt{3}}\frac{\Delta x}{\Delta t}$ represents the speed of sound in the lattice.]

$$f = \frac{\rho}{2\pi/3} e^{-\frac{3}{2}(\vec{e}\cdot\vec{e})} \left[1 + 3\,(\vec{e}\cdot\vec{u}) - \frac{3}{2}(\vec{u}\cdot\vec{u}) + \frac{9}{2}(\vec{e}\cdot\vec{u})^2\right] \tag{4.15}$$

$$f_k^{eq} = \rho\omega_k \left[1 + 3\,(\vec{e}\cdot\vec{u}) - \frac{3}{2}(\vec{u}\cdot\vec{u}) + \frac{9}{2}(\vec{e}\cdot\vec{u})^2\right] \tag{4.16}$$

where ω_k is the weighing factor given as;

$$w_i = \begin{cases} 4/9 & i = 0 \\ 1/9 & i = 1, 2, 3, 4 \\ 1/36 & i = 5, 6, 7, 8 \end{cases} \tag{4.17}$$

4.2.3 Macroscopic Quantities

Now that we have a formulation for determining the time evolution of the particle distribution function f, we need to use it to determine macroscopic quantities which are of primary interest to us. This is fairly straightforward. In LBM macroscopic quantities are obtained by evaluating the hydrodynamic moments of the distribution fucntion. For density and momentum flux, in descretised velocity-space, the relations are defined as follows;

$$\rho(\vec{x}, t) = \sum_{i=0}^{8} f_i(\vec{x}, t) \tag{4.18}$$

$$\rho\mathbf{u} = \frac{1}{\rho}\sum_{i=0}^{8} f_i(\vec{x}, t)\vec{e_i} \tag{4.19}$$

$$\tag{4.20}$$

4.2.4 Boundary conditions

Boundary conditions are an important part of computational fluid dynamics being central to the stability and accuracy of any numerical solution. For the lattice Boltzmann method, the discrete particle distribution functions on the boundary have to be determined to reflect the appropriate macroscopic boundary conditions.

In the present implementation, bouncback condition was implemented at the gloabal boundaries(walls) to model no slip as also at the interface between the solid and the melt phases. Zhou-He boundary condition was implemented at the inlet and the outlet nodes to model conditions for pipe flow.

Validating the phasefield model

5.0.5 Gibb's Thompson Effect

Our functional has the form of

$$\mathcal{F} = \int_{-\infty}^{\infty} (\gamma\epsilon|\nabla\phi|^2 + \frac{\gamma}{\epsilon}9\phi^2(1-\phi)^2 + ...)dV$$

By the equipartition of energy, we have for one dimension,

$$\begin{aligned} \gamma\epsilon\left(\frac{\partial\phi}{\partial x}\right)^2 &= \frac{\gamma}{\epsilon}9\phi^2(1-\phi)^2 \\ \Rightarrow \frac{\partial\phi}{\partial x} &= \frac{3}{\epsilon}\phi(1-\phi) \end{aligned}$$

Also, we know that total surface energy σ is given by the interfacing the interfacial energy term over the entire domain,

$$\begin{aligned} \sigma &= \int_{-\infty}^{\infty} 2\gamma\epsilon\left(\frac{\partial\phi}{\partial x}\right)^2 \cdot dx \\ &= \int_0^1 2\gamma\epsilon\left(\frac{\partial\phi}{\partial x}\right) \cdot d\phi \\ &= 6\gamma\int_0^1 2\phi(1-\phi)d\phi \\ &= 6\gamma\left[\frac{\phi^2}{2} - \frac{\phi^3}{6}\right]_0^1 \\ &\Rightarrow \sigma = \gamma \end{aligned}$$

We also know that at critical radius, surface energy equals the driving force for solidification- due to deviation of deviation from equilibrium of the Free energy,

$$\frac{\sigma}{r} = (k-1)\mu\left(\mu - \mu_e q\right)$$

Thus, for a given radius we can calculate a critical μ_c for which the nuclei is stable. For $\mu > \mu_c$ nuclei should grow, otherwise the nuclei should shrink. We used the above relation to calculate the critical μ_c for a radius of 50 units and found out that this Gibbs Thompson relation indeed holds for the present model.

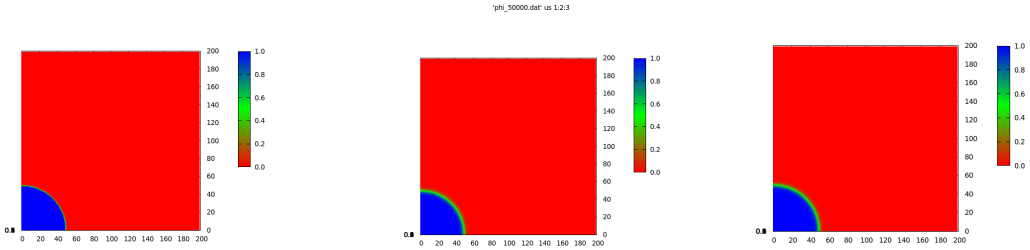

(a) timestep 0 (b) timestep 50000 (c) timestep 150000

Figure 5.1: Nuclei at critical radius - not growing

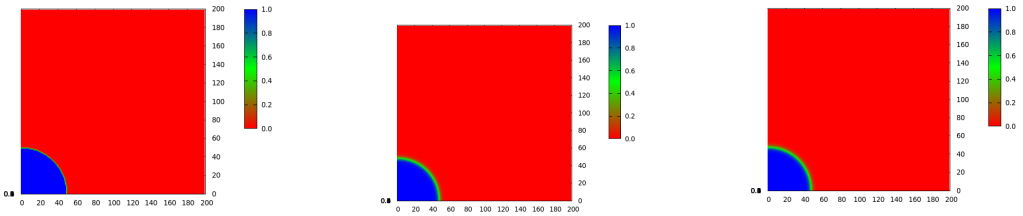

(a) timestep 0 (b) timestep 50000 (c) timestep 150000

Figure 5.2: Nuclei Shrinking - μ less than critical

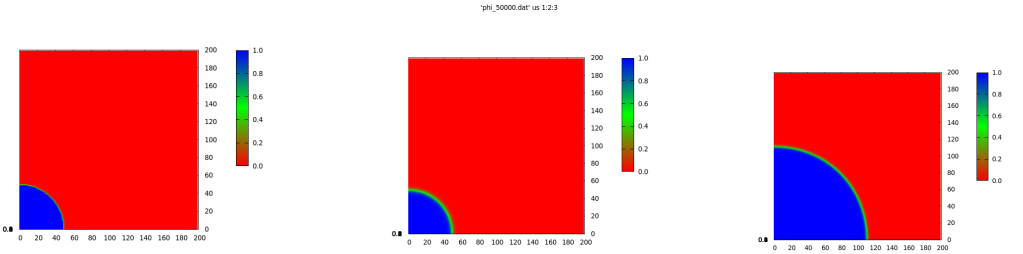

(a) timestep 0 (b) timestep 50000 (c) timestep 99000

Figure 5.3: Nuclei growing - μ greater than critical

5.0.6 Purturbation Analysis

The Mullins-Sekerka instability analysis gives a closed form analytical expression for sinusoidal purtubation of the plane front solution.

The expression takes the following form;

$$\frac{\dot{\delta}}{\delta} = V\tilde{\omega}\left[-\frac{b}{G} + \frac{1}{\tilde{\omega}}\left(k_\omega - \frac{V}{D}\right)\right]$$

$$\text{where, } \tilde{\omega} = k_\omega - \frac{V}{D}(1-k)$$

$$b = \frac{\Gamma\omega^2}{\mu_{eq}(1-k)}$$

$$\text{and } k_\omega = \frac{V}{2D} + \sqrt{\left(\frac{V}{2D}\right)^2 + \omega^2}$$

Where V is the velocity of the solidification front, D is the solute diffusivity in the melt phase, Γ is the Gibbs Thompson coefficient, ω is the frequency of perturbation, δ is the amplitude of perturbation and $\dot{\delta}$ is the rate at which the amplitude is changing.

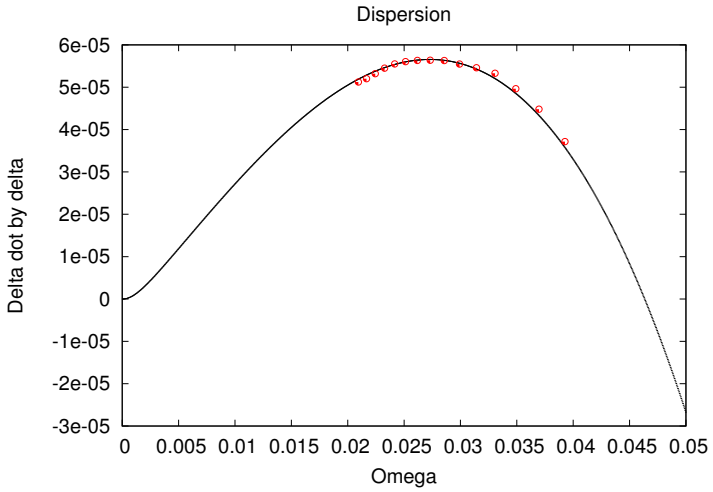

(a) dispersion plot

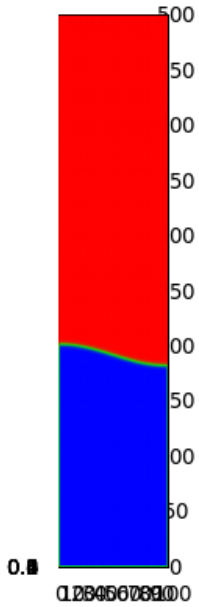

(b) sinusoidal ϕ front

Results

6.1 One Dimensional Solidification Profile

As a first test of the model, we tried to simulate solidification in one dimension for which the evoltuion profiles for state variables are well known. Mass transport is through diffusion only. The evolving profiles of the phasefield vatiable, ϕ, concentration and diffusion potential μ are depicted in the following images.

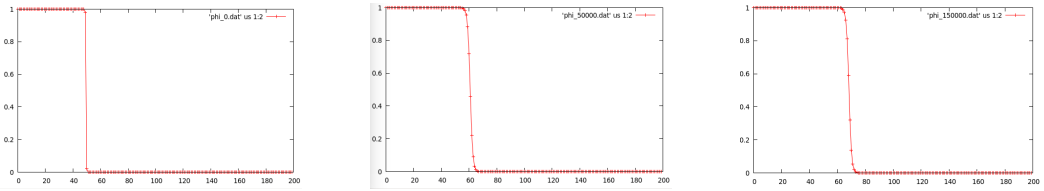

(a) timestep 0 (b) timestep 50000 (c) timestep 150000

Figure 6.1: time evolution of the phase field variable ϕ

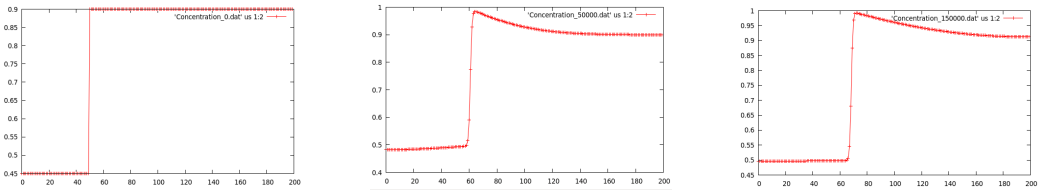

(a) timestep 0 (b) timestep 50000 (c) timestep 150000

Figure 6.2: time evolution of concentration

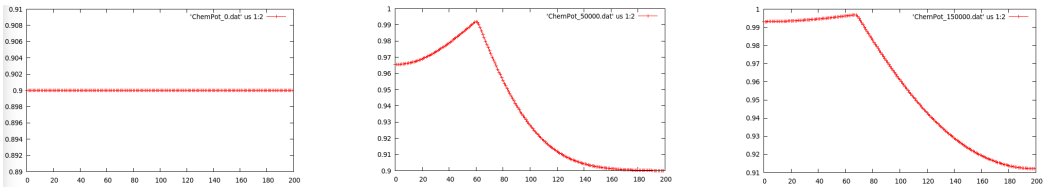

(a) timestep 0 (b) timestep 50000 (c) timestep 150000

Figure 6.3: time evolution of chemical potential μ

6.2 Anisotropic Solidification in 2D - only diffusion

Following images depict the ϕ profile during anisotropic solidification at different time steps.

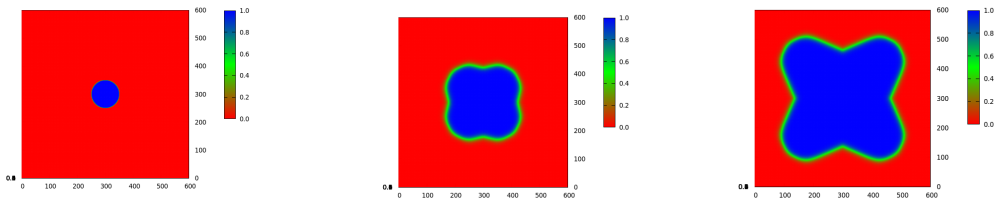

(a) timestep 0 (b) timestep 15000 (c) timestep 30000

Figure 6.4: Dendritic solidification on introducing anisotropy

6.3 Phasefield - Navier Stokes

Poiseuille flow

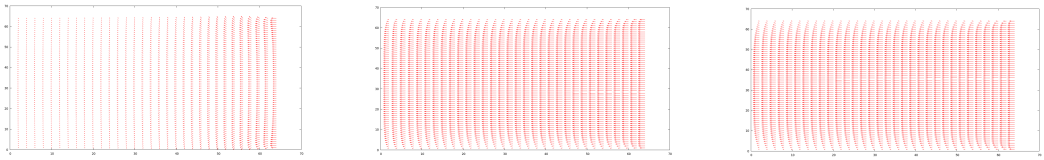

(a) timestep 1000 (b) timestep 10000 (c) timestep 50000

Figure 6.5: Pressure difference between East and West walls

Flow around a solid object in a closed space

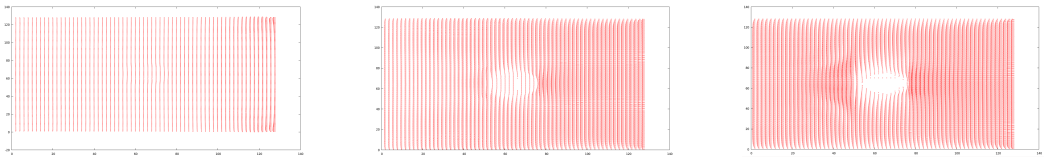

(a) timestep 1000 (b) timestep 10000 (c) timestep 50000

Figure 6.6: Flow around a solid with a diffuse interface

Anisotropic growth during fluid flow

Following images depict the evolution of the flow profile [left to right] and the solid phase over time.

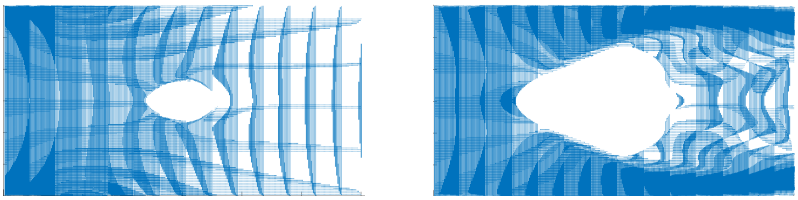

(a) timestep 20000 (b) timestep 65000

Figure 6.7: Forced Covection; left to right around evolving solid phase

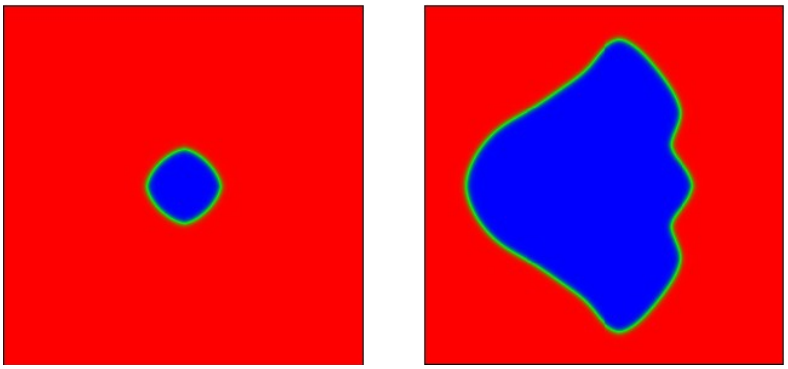

(a) timestep 20000 (b) timestep 65000

Figure 6.8: Evolving solid phase

6.4 Phasefield - Lattice Boltzmann

Having incorporated the lattice-Boltzmann based flow solver described earlier into our phasefield solver for solidification, we validated the solver by simulating the lid driven cavity flow and got expected results as seen in figure a.

Thereafter, we simulated anisotropic growth in presence of forced pipe flow [left to right] resulting in μ profiles as seen in figure b and figure c.

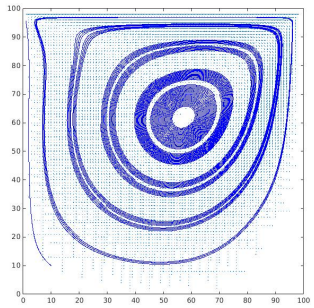

(a) lid driven cavity

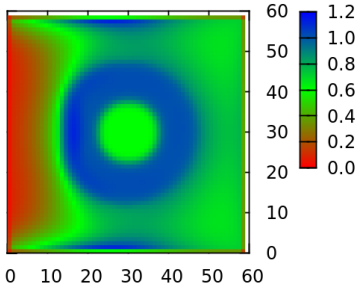

(b) mu field

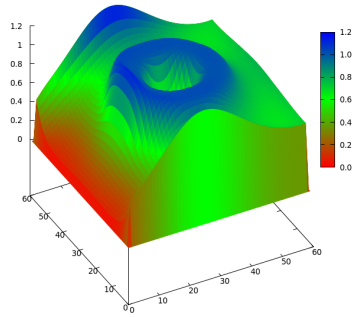

(c) mu field

Figure 6.9: Examples of flow profiles generated using lbm

Conclusion

Bibliography

[1] J.S. Langer, in Chance and Matter edited by J. Souletie, J. Vannenimus and R Stora (North Holland, Amsterdam 1987), p. 629; D Kessler, J Koplik and H Levine, Adv. Phys. 37, 255 (1988); E .A. Brenner and V.I. Mel'nikov, *ibid.* 40, 53 (1991)

[2] J. S. Langer, Phys. Rev. Lett., Volume 44, Number 15, 14 April 1980

[3] I. Steinbach, Acta Materialia 57 (2009) 2640 - 2645

[4] Tong et al., Phys. Rev. E, vol. 61, No. 1, January 2000

[5] Abhik Chaudhary and Britta Nestler, Phys. Rev. E 85,021602 (2012)

[6] Britta Nestler and Abhik Chaudhary, Current Opinion in solid State and Materials Science 15(2011) 93-105

[7] C. Beckermann et al., Jour. of Comp. Phys. 154, 468-496 (1999)

[8] W.J. Boettinger el al., Annu. Rev. Mater. Res. 2002. 32:163-94

[9] Yuanxun Bill Bao & Justin Meskas, "Lattice Boltzmann Model for Fluid Simulations", April 14, 2011

[10] Igor Mele, "Lattice Boltzmann method", March 2013

[11] Zou & He, "On pressure and velocity boundary conditions for the lattice Boltzmann BGK model", *Phys. Fluids*, **9**(6), June 1997

[12] Britta Nestler, Ali Aksi, Michael Selzer, "Combined lattice Boltzmann and phase-field simulations for incompressible fluid flow in porous media", *Mathematics and Computers in Simulation*, 80(2010) 1458-1468